


## Article

# Study on a New Type of Ventilation System for Rural Houses in Winter in the Severe Cold Regions of China

Baogang Zhang <sup>1,\*</sup>, Xianglu Cai <sup>1</sup>  and Ming Liu <sup>2</sup>

<sup>1</sup> Faculty of Infrastructure Engineering, Dalian University of Technology, Dalian 116081, China; caixianglu@mail.dlut.edu.cn

<sup>2</sup> School of Architecture and Fine Art, Dalian University of Technology, Dalian 116081, China; liuming@dlut.edu.cn

\* Correspondence: zhangbaogang@dlut.edu.cn or zhangbaogangtj@163.com

**Abstract:** The weather in the high latitudes of China is cold in winter. The pollution caused by the burning of biomass fuels used in rural individual heating is a great threat to human health. This study finds that the amounts of CO<sub>2</sub>, CO, PM<sub>2.5</sub>, and PM<sub>10</sub> in the bedroom exceed the standard and the temperature does not meet the standard based on indoor air measurements in rural residential buildings in Liaoning Province in winter. In this study, a mechanical ventilation method which uses flue gas to preheat fresh air is proposed, for the purpose of simultaneously improving the indoor air quality and the thermal environment of rural houses. The flue gas–fresh air heat exchange (FGFAHE) experiment shows that biomass combustion flue gas can increase the outdoor air temperature by 23.7 °C on average. The ventilation experiment shows that the method of mechanical ventilation combined with external window penetration can increase the dilution rate of indoor CO by more than 1 times. The simulation results of six different ventilation schemes show that the ventilation mode of the diagonal opposite side upper air supply and lower exhaust air (DOUSLE) has the best effect on indoor CO prevention and control, and the mode of median air supply is the most beneficial to the indoor thermal environment.



**Citation:** Zhang, B.; Cai, X.; Liu, M. Study on a New Type of Ventilation System for Rural Houses in Winter in the Severe Cold Regions of China. *Buildings* **2022**, *12*, 1010. <https://doi.org/10.3390/buildings12071010>

Academic Editors: Yue Wu, Zheming Liu and Zhe Kong

Received: 19 May 2022

Accepted: 11 July 2022

Published: 14 July 2022

**Publisher's Note:** MDPI stays neutral with regard to jurisdictional claims in published maps and institutional affiliations.



**Copyright:** © 2022 by the authors. Licensee MDPI, Basel, Switzerland. This article is an open access article distributed under the terms and conditions of the Creative Commons Attribution (CC BY) license (<https://creativecommons.org/licenses/by/4.0/>).

**Keywords:** rural houses; winter; ventilation; waste heat recover; air quality

## 1. Introduction

In the rural areas of China's severe cold regions, it is difficult to apply central heating due to factors such as population density and living habits [1]. Traditional individual heating is still the main means of heating houses. Inexpensive biomass fuels such as straw and firewood have been widely used until now [2]. According to the statistics, the total amount of bioenergy produced in rural areas of China is about 6 million tons per year, of which about 60% is used for heating and cooking [3]. The heating and cooking activities of individual farmers often produce a large quantity of pollutants, which seriously pollute the indoor air and pose a great threat to human health [4]. Studies have shown that long-term exposure to the environment containing biomass combustion fumes can cause coughing, asthma and other respiratory diseases [5], and it is especially harmful to pregnant women and children [6]. There are also studies showing that PM<sub>2.5</sub> produced by biomass burning in farmhouses can increase blood pressure in residents [7]. According to the statistics, in Europe, PM pollution shortens human life expectancy by 8.6 months [8]. Therefore, it is necessary for residents living in rural houses to adopt appropriate ventilation strategies to improve indoor air quality.

In recent years, the problem of indoor air quality in rural residential buildings has attracted great attention. Relevant scholars have carried out a lot of research. Wang et al. [9] conducted a measurement on the indoor air quality in the heating season of farmhouses around Harbin City, Heilongjiang Province, China, and found that the air pollutants over the standard level included PM<sub>2.5</sub>, PM<sub>10</sub>, CO<sub>2</sub>, CO, SO<sub>2</sub> and NO<sub>x</sub>, etc. Additionally, there

is a linear correlation between the mass concentrations of different pollutants, as observed through statistical analysis. There are many factors affecting the indoor air quality of farmhouses. Zhang et al. [10] found that the indoor pollution level of rural houses is related to the living habits of people, indoor temperature, relative humidity, biomass fuel combustion and ventilation methods, etc. Gu et al. [11] found that PM<sub>2.5</sub> directly generated by burning straw and wood accounted for 52% and 37% of the air in the room, and the indirectly generated PM<sub>2.5</sub> accounted for 7% and 15%. The indoor air pollutants in farmhouses also show different concentrations in different time and spaces. Yang [12] found that the indoor temperature, humidity and the concentration of air pollutants in rural residential buildings demonstrate similar regular changes every day during measurement. Liu [13] found that the concentration of indoor air pollutants in rural residential buildings is significantly different in winter and summer, and also in rooms with different functions. The above studies show that the indoor air pollution in rural residential buildings is characterized by a wide variety of air pollutants and is influenced by complex factors.

Ventilation is the most economical and practical way of removing indoor air pollutants [14]. A report on the indoor air quality of 85 buildings in the United States, Canada and Europe showed that improper ventilation is the biggest problem causing indoor air pollution [15]. A low ventilation rate can also cause a buildup in indoor moisture and provide growth conditions for mold and other microorganisms [16]. According to different air flow dynamics, ventilation can be divided into natural ventilation and mechanical ventilation [17]. Natural ventilation driven by thermal pressure and wind pressure [18] is the most important ventilation method in Chinese buildings at this stage. However, in the winter in severe cold regions, the temperature difference between indoor and outdoor environments can reach more than 30 °C, and improper ventilation can cause cold air intrusion, causing discomfort. Therefore, conventional natural ventilation methods are not suitable for farmhouses in cold regions. Passive ventilation based on solar energy and building waste heat, which can simultaneously increase ventilation rate and supply air temperature, has received extensive attention in recent years. A number of achievements has been made, including roof-mounted solar chimneys, wall-mounted solar chimneys [19], combination system of trombe walls, geothermal air pipes and a solar chimney [20], and a combination system of rotating heat recovery devices and rooftop wind catchers [21]. However, passive ventilation is often unstable due to uncontrollable solar radiation and outdoor air movement [22]. Several studies have shown that natural ventilation is not effective in removing pollutants from indoor air [23], and improper natural ventilation can even worsen air quality [24].

Compared with passive ventilation, mechanical ventilation can control the volume of the wind, and the starting and stopping of the ventilation, so as to regulate the microenvironment such as indoor airflow and air pressure [25]. Studies have shown that mechanical ventilation is better than natural ventilation at controlling pollutants such as particulate matter and fungi [26]. However, conventional mechanical ventilation can only control ventilation volume, and cannot change the air supply load. Indoor circulating air with supplementary air together can reduce the heat load of ventilation to a certain extent, but if the proportion of supplementary air is too low, the air quality of the supply air cannot be guaranteed [27]. Jinkyu et al. [28] found that when the volume ratio of supplementary air to recirculation air is adjusted to 1.2, the energy consumption can be reduced by about 22.1%, improving the indoor air quality at the same time. Underground duct ventilation uses the temperature of the soil to preheat the outdoor cold air, which has been widely used in Europe [29]. Zhao et al. [30] studied the application of a horizontal multi-row parallel underground pipeline ventilation system, and found that the system can preheat the outdoor air from −8~−10 °C to 0~15 °C. Wang et al. [31] conducted a survey of several houses in Sweden that had been reformed with combined ventilation heat recovery and low-temperature heating systems, and found that the comprehensive energy consumption and primary energy consumption were reduced by 55% and 22%, respectively, and the indoor air quality dissatisfaction rate dropped from 16.2% to 14.5%. Nonetheless, the above

methods can improve the supply air temperature to some extent, but the preheating effect is not obvious.

The average annual heating fuel consumption in rural areas in China is as high as 600 million tons, of which 60% is used for heating kang or stove-kang [32]. However, the heating efficiency of the kang system is low, the heat gain rate of the kang body is often lower than 50%, and the temperature at the exit of the chimney is as high as 343–363 K [33], which is a serious waste of energy. Some scholars have launched research to recover this part of the waste heat. Yu et al. [34] found that the wall can effectively absorb the waste heat of the flue gas and increase the wall temperature by conducting an experimental study on the chimney combination wall. Jin et al. [35] conducted research on a combined heating system of hanging kang and soil heating. The results show that the efficiency of this system is 21.26% higher than that of traditional floor-standing kang. Zhao [36] proposed a tunnel heating system with flue gas waste heat, and it was found that this system can save 9.17% of the heating energy consumption. The above studies all use the building envelope construction to absorb the waste heat of the combustion flue gas of farmhouses. Up to now, few people have carried out research on the heat exchange between flue gas and fresh air.

This study intends to explore the appropriate ventilation strategy according to the law of change of the indoor air pollutant concentration in the farmhouse using the waste heat of the flue gas emitted by the farmhouse stove and kang system (SKS) to preheat the outdoor fresh air and reduce the heat load at the same time, and. This scheme can simultaneously improve the indoor air quality and indoor thermal environment of rural houses in severe cold areas in China, and can recycle the waste heat resource, which has far-reaching significance for improving the living comfort and health level of rural residents and achieving sustainable development. In this study, we conduct a field measurement of indoor air in rural houses in severe cold areas in China, and summarizes the concentration changes; we also conduct a flue gas–fresh air heat exchange (FGFAHE) experiment to explore the preheating effect of smoke exhaust from the SKS of farmhouses on outdoor fresh air and the dilution effect of mechanical ventilation on indoor air pollutants in farmhouses. This study also adopts the simulation method to explore the best air supply and exhaust outlet layout scheme suitable for farmhouses in severe cold areas.

## 2. Indoor Air Measurement of Rural Houses in Western Liaoning, China

### 2.1. Materials and Methods

Reasonable ventilation should achieve maximum energy saving on the basis of effectively improving indoor air quality. For rural houses in severe cold areas, the concentration state of indoor air pollutants can be divided into different levels, and the purpose of precise air supply can be achieved by adjusting the ventilation volume according to the concentration level of pollutants. Therefore, it is necessary to grasp the concentration state and the changing regularities of indoor air pollutants in farmhouses. In this study, CO<sub>2</sub>, CO, PM<sub>10</sub>, PM<sub>2.5</sub>, formaldehyde, TVOC, temperature and relative humidity are measured for five consecutive days in the bedroom of three rural houses in Chaoyang City, Liaoning Province, China. The test instruments and the introductions are shown in Table 1.

**Table 1.** Introduction of test instrument.

Equipment	Model	Metrics	Range	Accuracy
Environmental monitor	Environmental monitor EVM serious	CO <sub>2</sub>	0~5000 ppm	±100 ppm
		CO	0~1000 ppm	±5%
		Temperature	−20~60 °C	±1.1 °C
		Relative humidity	0~100%	±5%
Particulate Monitor	LIGHTHOUSE3016	PM <sub>2.5</sub> PM <sub>10</sub>	0~4,000,000/ft <sup>3</sup>	±5%
Formaldehyde Monitor	AKBT-PID-CH2O	Formaldehyde	0~100 ppm	±0.01 ppm
TVOC Monitor	AKBT-PID-TVOC	TVOC	0~100 ppm	±0.01 ppm

The test time was from January 27 2021 to February 10 2021. The test method refers to “Indoor Air Quality Standards (GBT18883-2002)”.

## 2.2. Results and Discussion

The test results are shown in Figure 1. The white area in the figure represents the personnel activity period (PAP, 7:00–22:00), the purple area represents the nighttime sleep period (NSP, 22:00–7:00), and the red horizontal dotted line represents the safety limit in relevant standards.

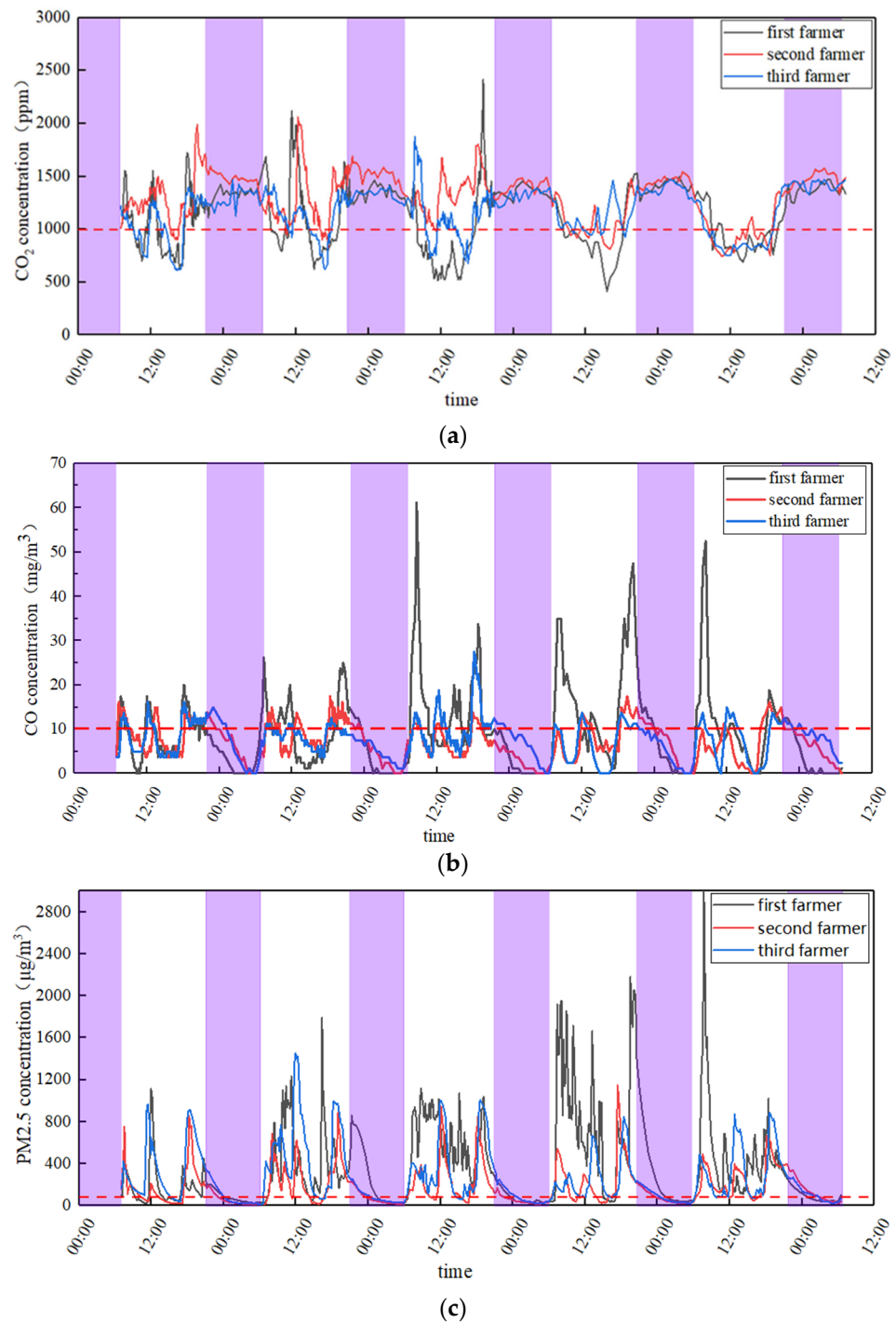


Figure 1. Cont.

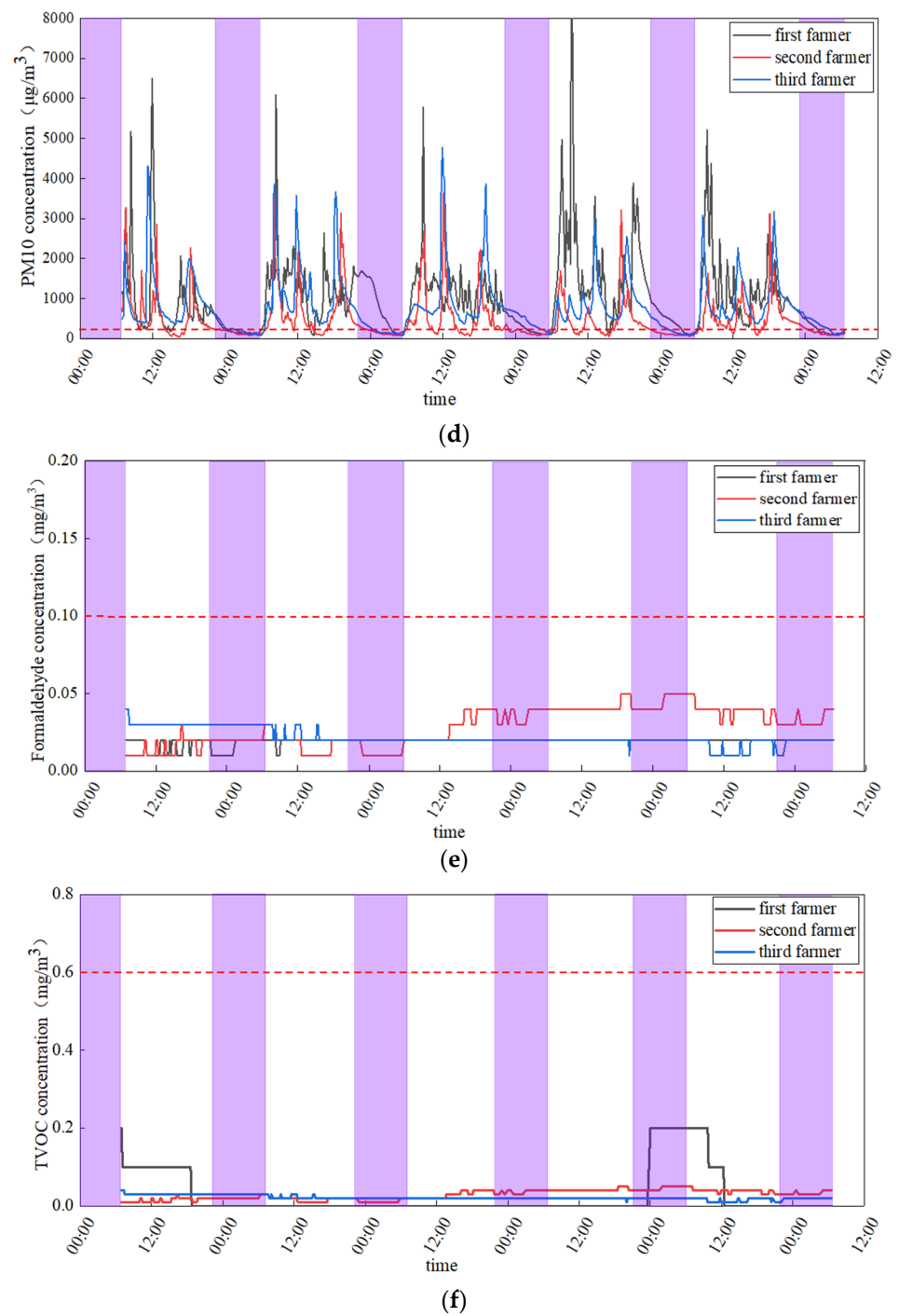
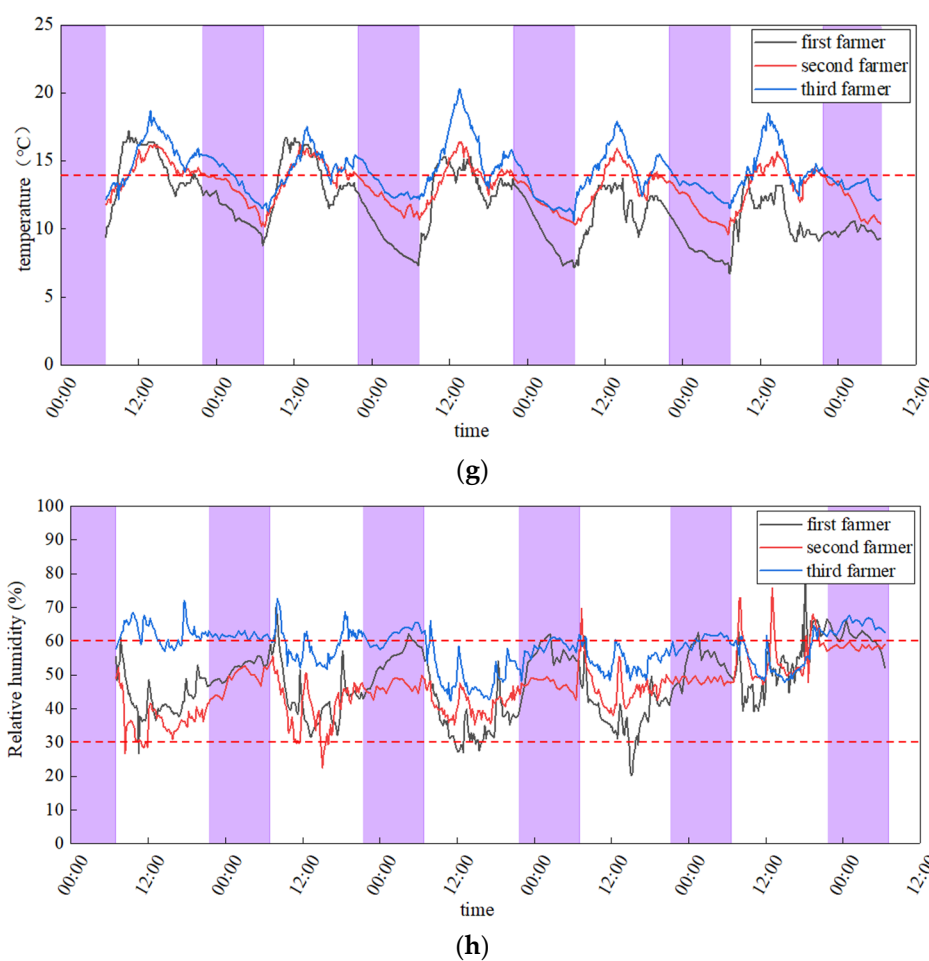


Figure 1. Cont.



**Figure 1.** Field test of air quality in bedrooms of three farmhouses for 5 consecutive days: (a) CO<sub>2</sub>, (b) CO, (c) PM<sub>2.5</sub>, (d) PM<sub>10</sub>, (e) Formaldehyde, (f) TVOC, (g) temperature, (h) relative humidity.

According to the above test, it can be found that during the test period, the relative humidity of the three farmhouse bedrooms is within the comfortable range most of the day, and it slightly deviates from the comfort zone for a short period of time. The concentrations of formaldehyde and TVOC are far below the standard values throughout the day. The concentration of CO<sub>2</sub> exceeds the standard value most of the time throughout the day, and it continues to be in a high concentration state during NSP, generally between 1000 ppm and 2000 ppm. The concentrations of CO, PM<sub>2.5</sub>, and PM<sub>10</sub> exceed the standard to varying degrees during PAP, and they gradually decrease during NSP and are within the standard value most of the time. The indoor temperature shows a trend of rising first and then falling during PAP, and gradually decreases during NSP. The average temperature throughout the day is lower than the winter calculation temperature of farmhouses stipulated in the “Design Standards for Energy Efficiency of Rural Residential Buildings (GBT 50824-2013)”.

Studies have shown that a high CO<sub>2</sub> concentration can reduce the cognitive performance and attention of building occupants [37]. The studies show that 10,000 ppm exposure for 30 min can cause respiratory toxicity in an adult [38]. An indoor CO<sub>2</sub> concentration in the range of 1000–2000 ppm generally causes drowsiness but no short-term health effects [12]. Therefore, the impact of CO<sub>2</sub> on people during bedtime may not be considered. The main factor that affects residents’ thermal comfort during NSP is the small-scale microenvironment around kang, and so the impact of comprehensive indoor air temperature at night may not be focused on. The critical period is PAP, and the key indicators are CO<sub>2</sub>, CO, PM<sub>2.5</sub>, PM<sub>10</sub> and temperature.

Observing the above curves, it can be found that the changes in CO<sub>2</sub>, CO, PM<sub>2.5</sub> and PM<sub>10</sub> concentrations in the bedrooms of the three farmhouses are disorderly, which

is caused by the irregular activities of indoor residents. However, in general, there is a common trend, in that there are some peaks exceeding the standard value during the daily cooking period. In addition, many local residents also report that the bedroom often produces a choking feeling of smoke during these periods.

It can be found that there are two main reasons for the severe indoor air pollution in rural houses observed through the on-site investigation. The first reason is the unreasonable layout of the rooms. The kitchen is the most polluted place in the farmhouses. However, most of the rural houses in this area have adjacent bedrooms and kitchens, which are connected by bedroom doors that are open all day. The door curtain made from cotton cloth on the bedroom doors cannot effectively prevent the spread of kitchen pollution into the room. The second reason is the poor smoke resistance of the building. The kang body is mainly composed of clay, which is different from the surrounding wall material and can easily cause improper connection, resulting in smoke leakage. The extremely high concentration of pollutants in the flue gas is bound to have an adverse effect on the indoor air. Cooking is the most important period of rural kitchen activities. The main reason for the serious pollution during the three meal periods is the large quantity of pollutants directly or indirectly produced by cooking activities that are released into the room.

According to statistics, the average CO<sub>2</sub> over-standard rates in the bedrooms of the three farmhouses are 45.7%, 84.9%, and 68.6%, respectively, and the average excess multiples are 1.01, 1.26, and 1.17. The average CO over-standard rates are 54.8%, 46.1%, and 48.1%, respectively. The average PM<sub>2.5</sub> over-standard rates are 85.8%, 77.4% and 82.6%, and the average exceeding multiples are 5.5, 2.89 and 4.2, respectively. The average PM<sub>10</sub> over-standard rates are 95.1%, 78.0% and 86.4%, and the average exceeding multiples were 7.5, 4.2 and 5.3, respectively. In view of the poor air quality in the bedrooms of farmhouses, it is necessary to take reasonable ventilation measures. The cooking periods should be taken as the key ventilation periods.

### 3. Experiment of the New Ventilation System

#### 3.1. Materials and Methods

Observing Figure 1g, it can be seen that the temperature level of the bedrooms of the three farmhouses is poor. In severe cold areas where the outdoor temperature is low in winter, introducing outdoor fresh air directly into the room would further damage the indoor thermal environment. This study seeks to use the flue gas emitted by the SKS in the farmhouses to preheat the outdoor air. The design of the flue gas–fresh air heat exchange (FGFAHE) experiment bench is shown in Figure 2. It is not advisable to set up exhaust vents in the experiment room because the room is surrounded by walls on three sides, and one side is adjacent to the kitchen. In this study, infiltration exhaust is selected. The schematic graph for the pipeline paths of the fresh air system is shown in Figure 3.

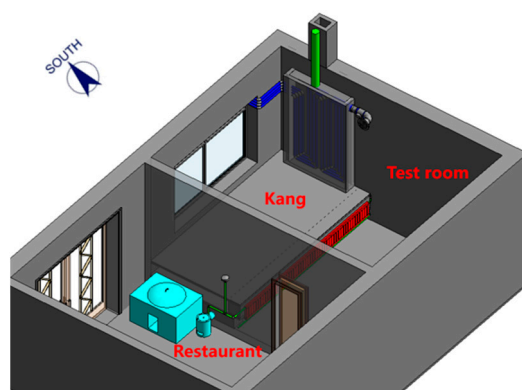
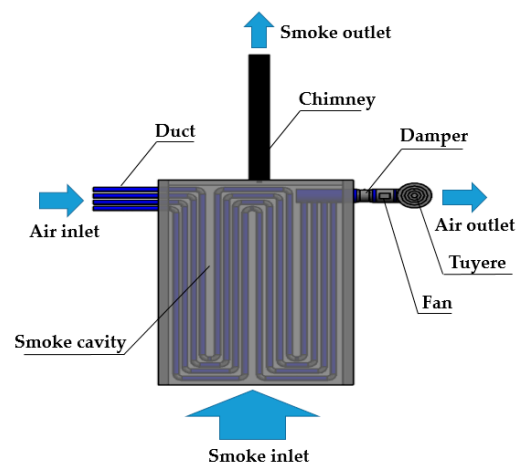


Figure 2. Design of FGFAHE experiment bench.



**Figure 3.** Schematic graph for the pipeline paths of the fresh air system.

The feasibility of the design scheme was demonstrated before the experiment bench was built. Considering the price, melting point, thermal conductivity and other aspects comprehensively, we chose a 304 stainless steel telescopic tube as the heat exchange air tube. Considering the size of the smoke cavity, the diameter of the air duct was preset to 50 mm. The size of the smoke cavity was  $1.2 \text{ m} \times 1.5 \text{ m} \times 0.3 \text{ m}$ , and the air ducts were arranged in parallel in a serpentine shape in the smoke cavity.

Fan selection is a very critical step. This study sought to check the resistance of the test system with a ventilation frequency of  $3 \text{ h}^{-1}$ . The size of the experiment room was  $4.5 \text{ m} \times 3.5 \text{ m} \times 3 \text{ m}$ . The calculation result of the ventilation volume in this state was about  $141.3 \text{ m}^3/\text{h}$ , and the air velocity was about  $5 \text{ m/s}$ . This was the state with the largest system resistance. The relevant local resistance coefficients refer to the second edition of the “Practical Heating and Air Conditioning Design Handbook” [39]. The resistance check results are shown in Table 2 below. It can be found from the table that the maximum resistance of the system was about  $274.6 \text{ Pa}$ . Taking the wind pressure correction coefficient as 1.2, the total resistance of the system was obtained as  $329.72 \text{ Pa}$ . A HF150 variable frequency duct fan with a rated power of  $57 \text{ w}$  was selected. Under the rated power, it could provide a static pressure value of  $330 \text{ pa}$  and a ventilation volume of  $650 \text{ m}^3/\text{h}$ , ensuring the normal operation of the system.

The outer wall of the smoke chamber of the experiment bench was made of red clay brick, and the connection between the air duct and the wall of the smoke chamber is smoothed with local high-viscosity laterite mud to avoid the infiltration of smoke. In order to avoid the influence of cold air entry caused by the poor sealing of the air duct and the outer window, this position was sealed with foam material, as shown in Figure 4.



**Figure 4.** FGFAHE experiment bench: (a) experiment bench’s appearance, (b) duct arrangement.



**Table 2.** Hydraulic calculation of fresh air system.

Pipe Number	Air Flow $Q_v/(m^3/h)$	Length L/m	Width a/mm	Height b/mm	Actual Cross-Sectional Area $S/m^2$	Tube Wind Speed $V_s/(m/s)$	Dynamic Pressure $P_d/Pa$	Coefficient of Local Resistance $\sum \xi$	Local Resistance $\Delta P_j/Pa$	Specific Frictional Resistance $R_m/(Pa/m)$	Frictional Drag $R_m L/Pa$	Section Resistance $(R_m L + \Delta P_j)/Pa$	Total System Resistance $\Delta P/Pa$	Allow for the Wind $p_t/Pa$
Main pipe	141.3	0.6	100	100	0.00785	5.00	15.00	1.77	26.55	1.20	0.72	27.27		
First branch	141.3 35.33	0.25 5.53	100 50	100 50	0.00785 0.0019625	5.00 5.00	15.00 15.00	0.20 1.40	3.00 21.00	1.20 6.00	0.30 33.15	3.30 54.15		
Second branch	105.98 35.33	0.08 5.36	100 50	100 50	0.00785 0.0019625	3.75 5.00	8.44 15.00	1.52 1.40	12.83 21.00	3.20 6.00	0.26 32.16	13.08 53.16	274.76	329.72
Third branch	70.65 35.33	0.08 5.17	100 50	100 50	0.00785 0.0019625	2.50 5.00	3.75 15.00	5.40 1.40	20.25 21.00	1.30 6.00	0.10 31.02	20.35 52.02		
Fourth branch	35.33 35.33	0.08 5.03	100 50	100 50	0.00785 0.0019625	1.25 5.00	0.94 15.00	0.20 1.40	0.19 21.00	1.00 6.00	0.08 30.16	0.27 51.16		

This study carried out a three-day experiment from 15 to 17 February 2021. The weather was sunny during the three days. The experiment time was in the morning, and the outdoor average air temperatures on the three days were: 15 February:  $-17\text{ }^{\circ}\text{C}$ , 16 February:  $-14\text{ }^{\circ}\text{C}$ , 17 February:  $-10\text{ }^{\circ}\text{C}$ .

The content of this experiment can be divided into two parts. The first part mainly discussed the heat exchange effect between flue gas and fresh air. The experiment was divided into two working conditions: the time of burning and one hour after the burning stopped. The flue gas temperature was measured with the TM902c thermometer. The average temperature of the flue gas at the entrance of the kang was  $150\text{ }^{\circ}\text{C}$  in the first working condition and  $50\text{ }^{\circ}\text{C}$  in the second working condition. During the experiment, the air velocity was controlled by adjusting the fan gear position and the air valve, and the change in the ventilation volume was reflected by the change in the air velocity. The TES1341 hot-wire anemometer was used to measure the temperature of fresh air outlet.

The second part of the experiment mainly discussed the dilution effect of fresh air on indoor CO. In this part, the stove was first fired to create a CO polluted environment in the room, and the environmental monitor (an EVM series environmental detector) was turned on to test the CO concentration. Before starting the experiment, the door was closed tightly and the fan was turned on for ventilation. Exhaust could be eliminated by the penetration of external windows. The air velocity was controlled to be  $5\text{ m/s}$ ,  $4\text{ m/s}$  and  $3\text{ m/s}$ , respectively (the corresponding fresh air volumes were  $141\text{ m}^3/\text{h}$ ,  $113\text{ m}^3/\text{h}$  and  $85\text{ m}^3/\text{h}$ , respectively) in 3 groups of experiments.

### 3.2. Results and Discussion

As shown in Figure 5, the results show that the flue gas can preheat the outdoor air from  $-17\text{ }^{\circ}\text{C}\sim-10\text{ }^{\circ}\text{C}$  to  $6\text{ }^{\circ}\text{C}\sim30\text{ }^{\circ}\text{C}$  during the time of burning. When the experiment ventilation volume reached the maximum ( $141\text{ m}^3/\text{h}$ ), the system raises the outdoor air temperature by  $7.2\text{ }^{\circ}\text{C}$  on average. When the experiment ventilation rate was the minimum ( $29\text{ m}^3/\text{h}$ ), the system could raise the outdoor air temperature by an average of  $23.7\text{ }^{\circ}\text{C}$ . In the working period of one hour after the burning stopped, the residual heat in the smoke chamber preheated the outdoor cold air to  $-6\text{ }^{\circ}\text{C}\sim10\text{ }^{\circ}\text{C}$ .

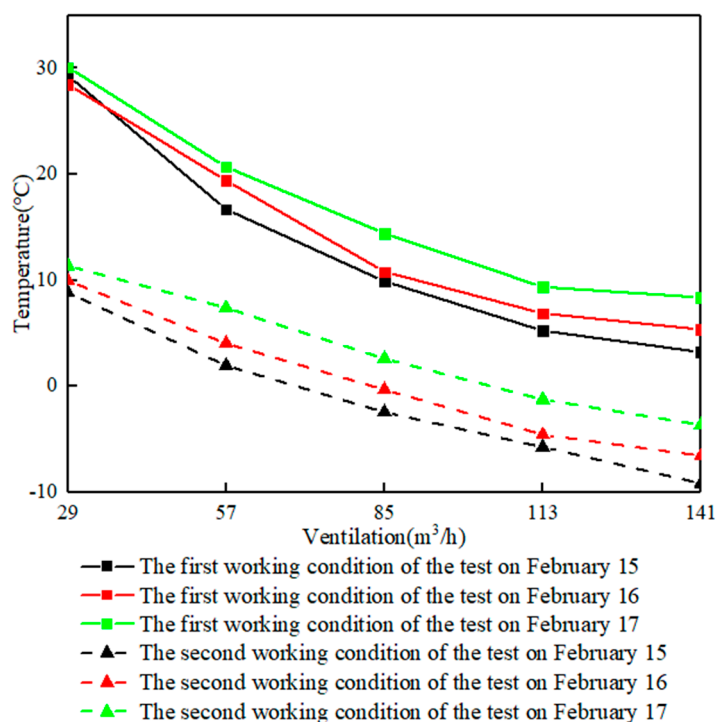


Figure 5. Fresh air preheating experiment results.

The change in indoor CO concentration of the three groups without any ventilation measures was selected as a comparison, and the curve of CO concentration with time was drawn, as shown in Figure 6. The experiment results show that the combination of mechanical ventilation and external window penetration could effectively dilute indoor air pollutants, and the dilution rate was more than double that of natural penetration. When the ventilation rate was 85~141 m<sup>3</sup>/h, it only took about 17–30 min to reduce the CO concentration of 20~25 mg/m<sup>3</sup> to below the standard value (10 mg/m<sup>3</sup>).

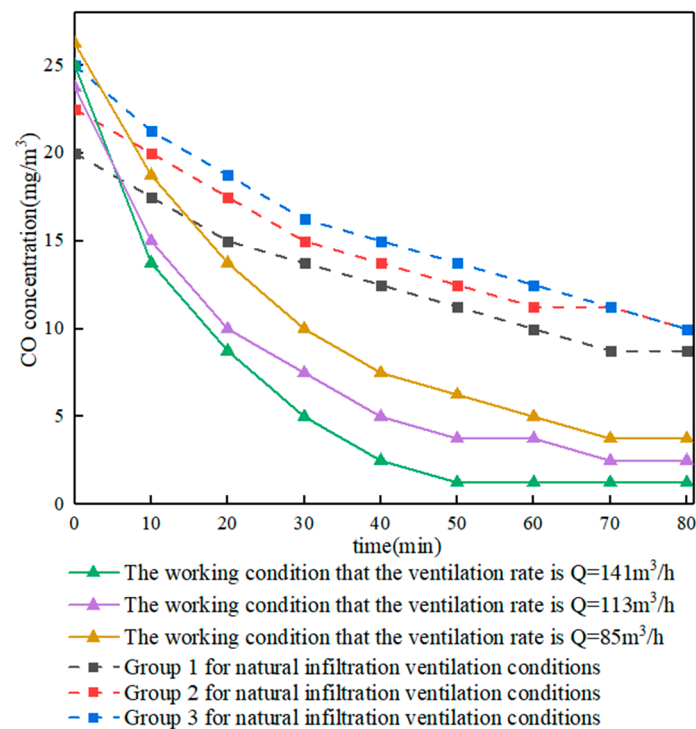


Figure 6. Fresh air dilution experiment results.

For mechanical ventilation, reasonable airflow organization design is the key to achieving efficient ventilation. The above experiments only explore the ventilation effect of one scheme (combination of mechanical ventilation and exterior window penetration). According to the characteristics of the experiment room and the bench, it is not appropriate to adjust the position of the air supply port or add additional exhaust ports to conduct more experiments. Therefore, it is necessary to adopt the method of simulation to discuss more schemes.

## 4. Simulation of the New Ventilation System

### 4.1. Methods

In this study, ANSYS FLUENT software was selected for the simulation of pollutant dispersion and flow field analysis. A CFD model was established first, and it was necessary to verify the accuracy of the model with the above experiments. The exhaust method of the above ventilation experiment was the penetration of external window, and so it was necessary to clarify the size of the penetration gap. In this study, CO was used as the tracer gas. The volume of the gap was determined by the CO natural penetration experiment, the procedure of which is as follows.

First, we opened the door to connect the experiment room with the kitchen, and started a fire on the stove to create a high-concentration CO environment in the room. Then, we turned on the environmental detector to test the CO concentration and air temperature in the experiment room. We turned off the flame completely and closed the stove door when the CO concentration in the experiment room reached 25 ppm. We prepare the experiment when the CO concentration of the kitchen and the experiment room were similar for the

purpose of eliminating the influence of mutual penetration on the experiment. We recorded the concentration of CO at the time when the experiment started. After about 2–3 h, the experiment ended when the CO in the room was sufficiently diluted. We carried out three experiments and derived the results. Then, we plotted the change curve of CO concentration with time, as shown in Figure 6 for natural infiltration ventilation conditions.

The time taken for the CO concentration to decrease from 20 mg/m<sup>3</sup> (16 ppm) to 10 µg/m<sup>3</sup> (8 ppm) in the three experiments was 61 min, 66 min and 71 min, respectively. The average dilution time of 66 min was taken to calculate the permeation ventilation. The size of the kang was 3.5 m × 2.0 m × 0.7 m, and the effective space size of the experiment room was 42.35 m<sup>3</sup>. According to the above conditions, the natural penetration ventilation volume was obtained as Q = 38.5 m<sup>3</sup>/h.

The main driving force of infiltration ventilation is the thermal pressure formed by the temperature difference between indoor and outdoor. The formula for the calculation of hot pressure [40] is as follows:

$$\Delta P_t = (\rho_w - \rho_n)gh \quad (1)$$

where  $\Delta P_t$  is the level of the hot pressure, Pa;  $\rho_w$  is the outdoor air density at the experiment time, kg/m<sup>3</sup>;  $\rho_n$  is the indoor air density at the experiment time, kg/m<sup>3</sup>; and  $h$  is the net height difference between the supply and exhaust air, m.

The calculation of natural ventilation dynamic pressure is shown as follows [40].

$$\Delta P_v = \xi \frac{v^2}{2} \rho \quad (2)$$

where  $\Delta P_v$  is the pressure difference between the two sides of the window hole, Pa;  $v$  is the flow velocity of the air flowing through the window hole, m/s;  $\rho$  is the density of the air passing through the window hole, kg/m<sup>3</sup>; and  $\xi$  is the local resistance coefficient of the window hole.

The size of the outer window of the experiment room is 1.5 m × 1.5 m. Taking the half plane of the window height as the neutral plane, then the average height of air supply and exhaust is 0.75 m. In the three natural infiltration experiments, the average outdoor temperature was −12 °C and the average indoor temperature was 10 °C. Air density refers to Appendix 5 in the textbook “Heat Transfer” published by China Higher Education Press. The above data are substituted into (1) to obtain the hot pressure size as  $\Delta P_t = 0.57$  Pa. The thermal pressure is converted into dynamic pressure of natural infiltration, that is,  $\Delta P_t = \Delta P_v$ . The local resistance coefficient of the window hole refers to the vertical axis plate window in the textbook “Ventilation Engineering” published by China Machinery Industry Press. The above data are substituted into (2) to obtain the infiltration velocity as  $v = 0.6$  m/s. Then, the gap area of the outer window can be obtained as 0.018 m<sup>2</sup>. The total length of the slit (openable part) is 6.6 m through measurement, so the average width of the outer window slit is 5.39 mm.

The natural infiltration process is slow. Due to the lack of room insulation measures, the indoor temperature will gradually drop during the experiment. Therefore, the result obtained by the above method is greater than the actual value. Then, a certain degree of correction should be carried out. Taking the convenience of calculation into consideration, the gap width of this model is set to 5 mm after correction. The average width of sliding window gaps in China are about 2–4 mm, which is reasonable for rural buildings with poor construction technology.

The experiment platform is geometrically modeled by ICFM CFD software, as shown in Figure 7. The following assumptions are made to facilitate problem analysis. First, air is an incompressible fluid, and the viscous dissipation in the flow process should be ignored; second, the physical parameters of air do not change with temperature, and the density satisfies the Boussinesq assumption; third, the temperature of the envelope structure is uniform and stable; fourth, there are no other sources of CO pollution and infiltration in the room; fifth, the infiltration of the room only occurs in the external windows. In the

experiment room, the air flows under the disturbance of mechanical supply air, which is turbulent flow under forced convection. The control equations established in this study are as follows:

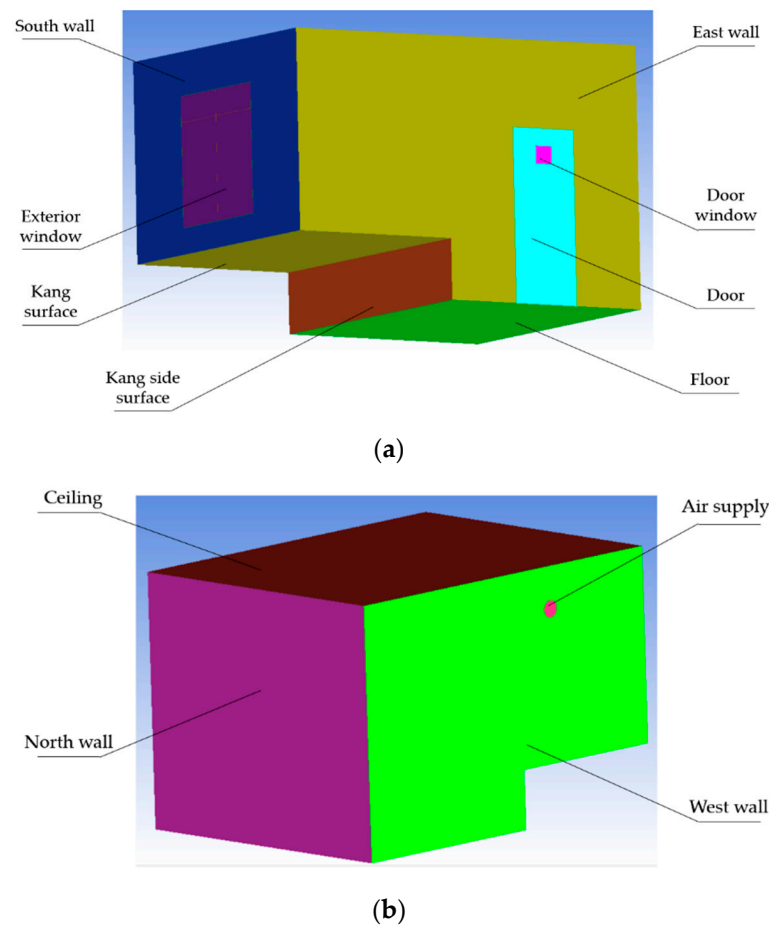


**Figure 7.** The geometric model of the experiment room, (a) southeast view, (b) Northwest view.

Continuity Equation

$$\frac{\partial u}{\partial x} + \frac{\partial v}{\partial y} + \frac{\partial w}{\partial z} = 0 \quad (3)$$

Momentum conservation equation

$$\rho u \frac{\partial u}{\partial x} + \rho v \frac{\partial u}{\partial y} + \rho w \frac{\partial u}{\partial z} = \mu \left( \frac{\partial^2 u}{\partial x^2} + \frac{\partial^2 u}{\partial y^2} + \frac{\partial^2 u}{\partial z^2} \right) - \frac{\partial p}{\partial x} \quad (4)$$

$$\rho u \frac{\partial v}{\partial x} + \rho v \frac{\partial v}{\partial y} + \rho w \frac{\partial v}{\partial z} = \mu \left( \frac{\partial^2 v}{\partial x^2} + \frac{\partial^2 v}{\partial y^2} + \frac{\partial^2 v}{\partial z^2} \right) - \frac{\partial p}{\partial y} - \rho g \quad (5)$$

$$\rho u \frac{\partial w}{\partial x} + \rho v \frac{\partial w}{\partial y} + \rho w \frac{\partial w}{\partial z} = \mu \left( \frac{\partial^2 w}{\partial x^2} + \frac{\partial^2 w}{\partial y^2} + \frac{\partial^2 w}{\partial z^2} \right) - \frac{\partial p}{\partial z} \quad (6)$$

Energy conservation equation

$$\rho c_p \left( u \frac{\partial T}{\partial x} + v \frac{\partial T}{\partial y} + w \frac{\partial T}{\partial z} \right) = \lambda \left( \frac{\partial^2 T}{\partial x^2} + \frac{\partial^2 T}{\partial y^2} + \frac{\partial^2 T}{\partial z^2} \right) + S_H \quad (7)$$

Species mass-conservation equation

$$\frac{\partial(\rho c_s)}{\partial t} + \frac{\partial(c_s u)}{\partial x} + \frac{\partial(c_s v)}{\partial y} + \frac{\partial(c_s w)}{\partial z} = \frac{\partial}{\partial x} \left( D_s \frac{\partial(c_s)}{\partial x} \right) + \frac{\partial}{\partial y} \left( D_s \frac{\partial(c_s)}{\partial y} \right) + \frac{\partial}{\partial z} \left( D_s \frac{\partial(c_s)}{\partial z} \right) \quad (8)$$

In the formula,  $u$ ,  $v$ , and  $w$  represent the velocity of air in the  $X$ ,  $Y$ , and  $Z$  directions, respectively,  $m/s$ ;  $\rho$  is the density of the air,  $kg/m^3$ ;  $p$  is the pressure of the air,  $Pa$ ;  $\mu$  is the dynamic viscosity,  $Pa\cdot s$ ;  $c_p$  is the specific heat capacity at constant pressure,  $J/(kg\cdot K)$ ;  $T$  is the temperature of the gas,  $^{\circ}C$ ;  $\lambda$  is the thermal conductivity of the gas,  $W/(m\cdot K)$ ;  $S_H$  is the radiation heat transfer term;  $c_s$  is the volume concentration of the component; and  $D_S$  is the diffusion coefficient of the component.

When choosing a turbulence model, it is necessary to consider its calculation accuracy, calculation time and the computing power of the CPU. In this study, three turbulence models, namely the standard  $k-\epsilon$  model, the RNG  $k-\epsilon$  model and the realizable  $k-\epsilon$  model, are used to numerically simulate the ventilation process. The calculation results show that the convergence rate of the standard  $k-\epsilon$  model is slow, and the error is large when calculating the non-uniform turbulence problem. The residual curve of the RNG  $k-\epsilon$  model oscillates seriously. Using the realizable  $k-\epsilon$  model can improve the convergence speed of the calculation and reduce the error. Therefore, the realizable  $k-\epsilon$  model is selected for simulation calculation.

The boundary condition of the air inlet adopts the velocity inlet, and the inlet air velocity and temperature refer to the above experiment conditions, as shown in Table 3 below. The boundary condition of the air outlet adopts the pressure outlet. The boundary condition of the wall adopts the first type. The wall temperature is tested by the TM902C thermometer, and the average value of the experiment results is taken as shown in Table 4. The measured results of initial CO concentration and indoor air temperature are shown in Table 5. The SIMPLE algorithm is used to solve the problem, the non-steady time step is 0.1, and the maximum time step is 10.

**Table 3.** Inlet boundary conditions for ventilation dilution simulations.

Test Conditions	Velocity (m/s)	Temperature ( $^{\circ}C$ )
$Q = 141\ m^3/h$	5	8.40
$Q = 113\ m^3/h$	4	9.38
$Q = 85\ m^3/h$	3	14.44

**Table 4.** Wall temperature boundary condition for ventilation dilution simulation.

Project	Exterior Wall	Exterior Window	Floor	Roof	Kang Surface	Kang Side
Temperature ( $^{\circ}C$ )	8.1	1.8	4.5	7.2	42.6	28.7

**Table 5.** Initial conditions for ventilation dilution simulations.

Test Conditions	CO Concentration ( $mg/m^3$ )	Temperature ( $^{\circ}C$ )
$Q = 141\ m^3/h$	25	10.6
$Q = 113\ m^3/h$	23.75	10.9
$Q = 85\ m^3/h$	26.25	11.2

The geometric model is shown in Figure 7. The type of grid is a structured grid. Five sets of structured grid schemes are established to verify the grid independence, and the grid numbers are 43,624, 61,470, 156,408, 428,400 and 1,051,612, respectively. The five schemes are simulated under the test conditions of  $Q = 141\ m^3/h$ . The inlet velocity and temperature are shown in Table 3, the temperature of each wall of the experiment room is shown in Table 4, and the initial CO concentration and initial temperature of the test room are shown in Table 5. The curve of indoor CO concentration with time is drawn as shown in Figure 8. It can be seen from the figure that there is a small difference between the simulation results when the grid number is 156,408 and 428,400, the maximum error is  $0.4\ mg/m^3$ , and the average error is only  $0.3\ mg/m^3$ . Therefore, when the number of grids is greater than

156,408, the accuracy of numerical calculation is no longer significantly improved, and 156,408 grids can be used for calculation. The result of grid division is shown in Figure 9.

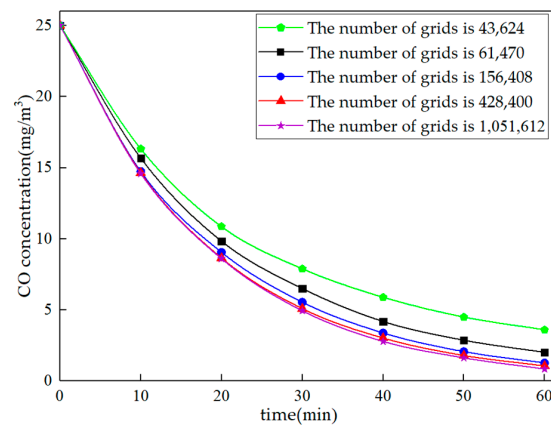


Figure 8. Grid independence verification.

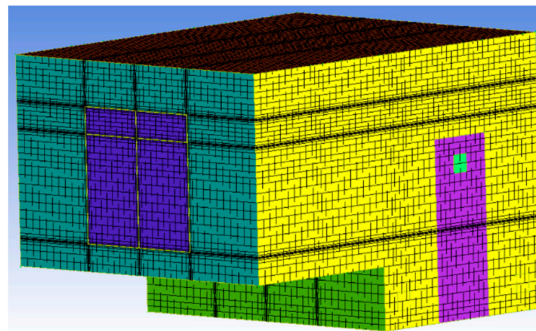


Figure 9. Structural meshing of room models.

The reliability of the model is verified by experiments with ventilation volume of  $Q = 141 \text{ m}^3/\text{h}$ ,  $Q = 113 \text{ m}^3/\text{h}$  and  $Q = 85 \text{ m}^3/\text{h}$ , respectively. The boundary conditions and initial conditions of each test are shown in Tables 3–5. The variation curve of the average CO concentration over time at a height of 1.2 m in the room is as shown in Figure 10. It can be seen from the figure that the errors between the simulation result and the experiment are small, of which the maximum error is  $0.98 \text{ mg}/\text{m}^3$ , and the average error is  $0.53 \text{ mg}/\text{m}^3$ . Therefore, it can be considered that the CFD model established in this study can represent the experimental results.

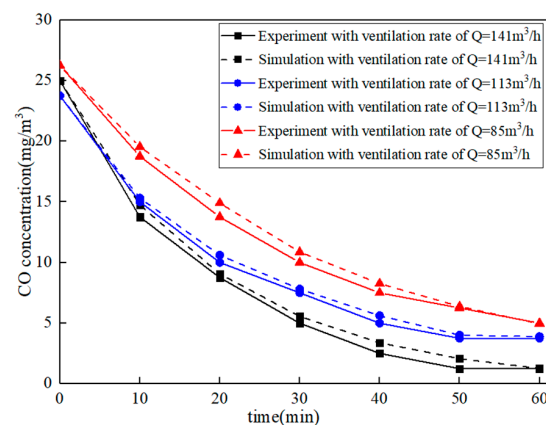
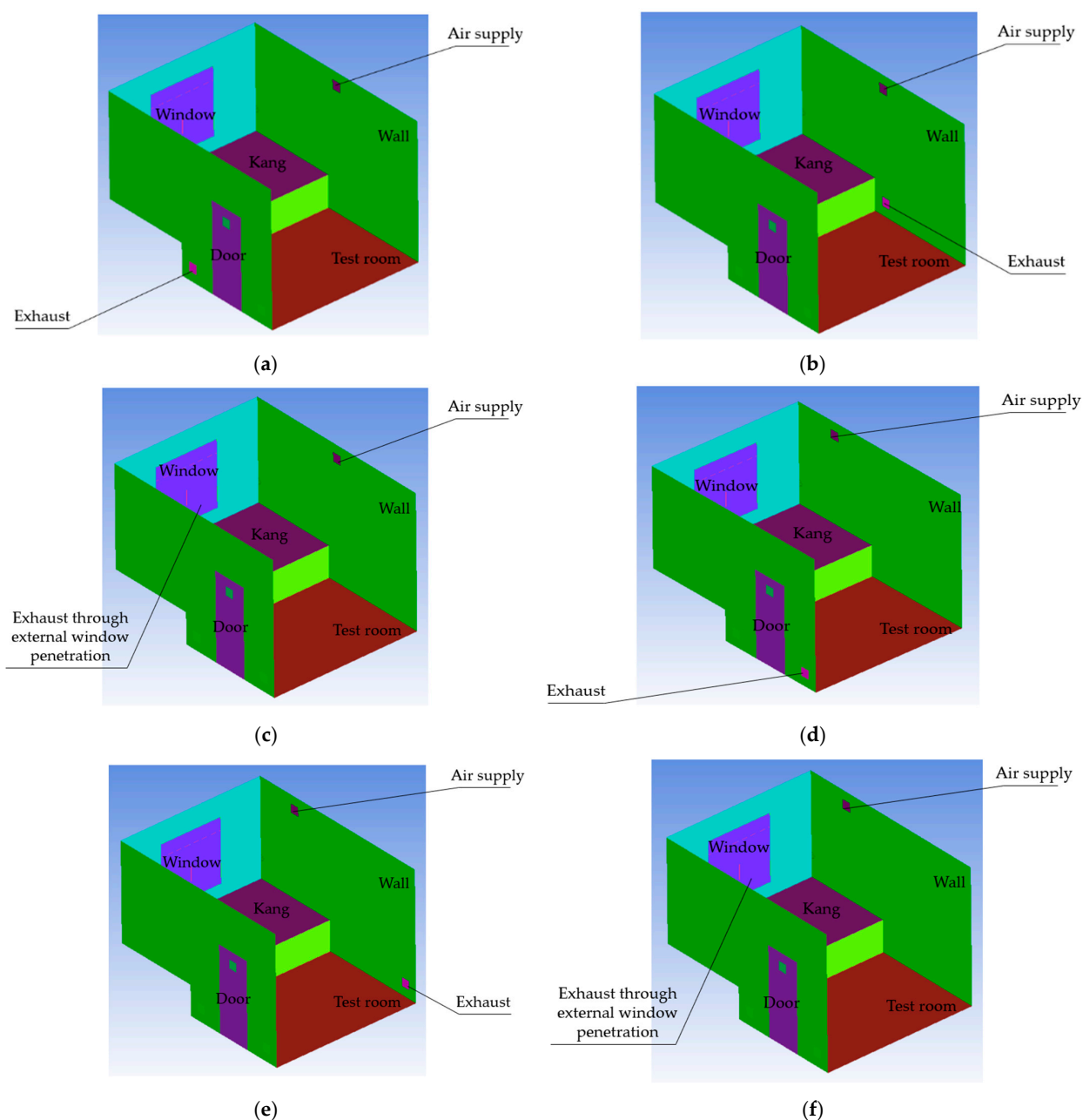


Figure 10. Model reliability verification.

The above model is now used to further explore the ventilation of different airflow organizations. According to the characteristics of rural houses and the relevant recommendations of “Design Code for Heating Ventilation and Air Condition (GB50736-2012)”, this study proposes six layout schemes of air supply and exhaust vents as follows: median opposite side upper air supply and lower exhaust air (MOUSLE), median same side upper air supply and lower exhaust air (MSUSLE), median upper air supply and exterior window penetration (MUSEWP), diagonal opposite side upper air supply and lower exhaust air (DOUSLE), diagonal same side upper air supply and lower exhaust air (DSUSLE), and diagonal upper air supply and exterior window penetration (DUSEWP). As shown in Figure 11. The simulation results of the six ventilation schemes are used as examples for discussion and analysis.



**Figure 11.** Six layout schemes of air supply and exhaust vents: (a) MOUSLE, (b) MSUSLE, (c) MUSEWP, (d) DOUSLE, (e) DSUSLE, (f) DUSEWP.



#### 4.2. Results and Discussion

The initial concentration of CO is set to  $25 \text{ mg/m}^3$ , and the data of the  $Q = 141 \text{ m}^3/\text{h}$  working condition of the above experiments are used as the boundary conditions to simulate the above six air supply and exhaust vents layout schemes. The calculation of average plane CO concentration at a height of 1.2 m in the room in the simulation results, and the CO concentration variation curves with time are as shown in Figure 12.

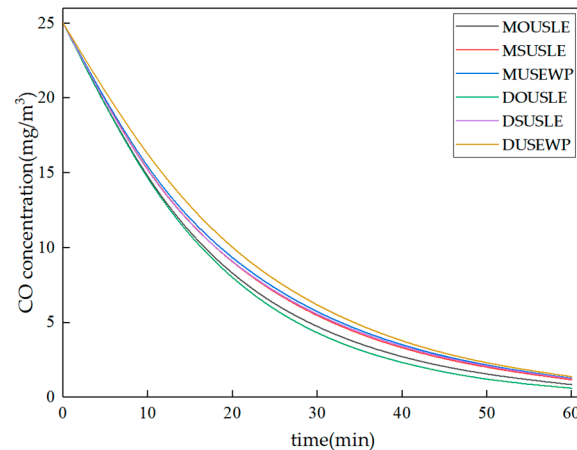


**Figure 12.** The curve of CO concentration changing with time in the room at a height of 1.2 m.

From the curve, we can see that all of the six schemes have a good dilution effect on indoor CO. The CO concentration in the room can be reduced from  $25 \text{ mg/m}^3$  to below the standard value ( $10 \text{ mg/m}^3$ ) within 20 min. The dilution rate is the fastest when the ventilation scheme is adopted with the DOUSLE, and the dilution time is 16.6 min. The dilution rate is the slowest when the ventilation is adopted with the DUSEWP, and the dilution time is 20.0 min.

Rural residents spend most of their time on the kang in the bedroom, so the environmental conditions around the kang should be focused. The CO concentration distribution contour is generated by intercepting the plane at a height of 1.2 m, as shown in Figure 13. From the contour, it can be found that when the ventilation mode of DOUSLE is adopted, the CO concentration level in the area where the kang is located is relatively low, and the area with a high CO concentration is mainly on the floor side. When adopting the mode of DUSEWP for ventilation, the CO concentration in the area where the kang is located is relatively high, which may be due to the fact that the air supply port is too close to the external window.

It can be seen from the FGFAHE experiment that with the increasing of ventilation volume, the supply air temperature gradually decreases. During the time of burning, when the fresh air volume is  $29 \text{ m}^3/\text{h}$ , the fresh air outlet temperature can reach  $3.24\sim 8.4 \text{ }^\circ\text{C}$ . According to the previous measurement, the average indoor temperature of rural house during PAP is  $13.2 \text{ }^\circ\text{C}$ . Therefore, if the FGFAHE system is used for ventilation, when the supply air volume is small, the supply air temperature can be higher than indoor air temperature, which is beneficial to the thermal environment of the bedroom; when the air supply volume is large, the air supply temperature can be lower than the indoor air temperature, which will destroy the thermal environment of the bedroom. In the following section, the indoor thermal environment is discussed by means of simulation in two cases of high ventilation ( $Q = 141 \text{ m}^3/\text{h}$ ) and low ventilation ( $Q = 29 \text{ m}^3/\text{h}$ ).

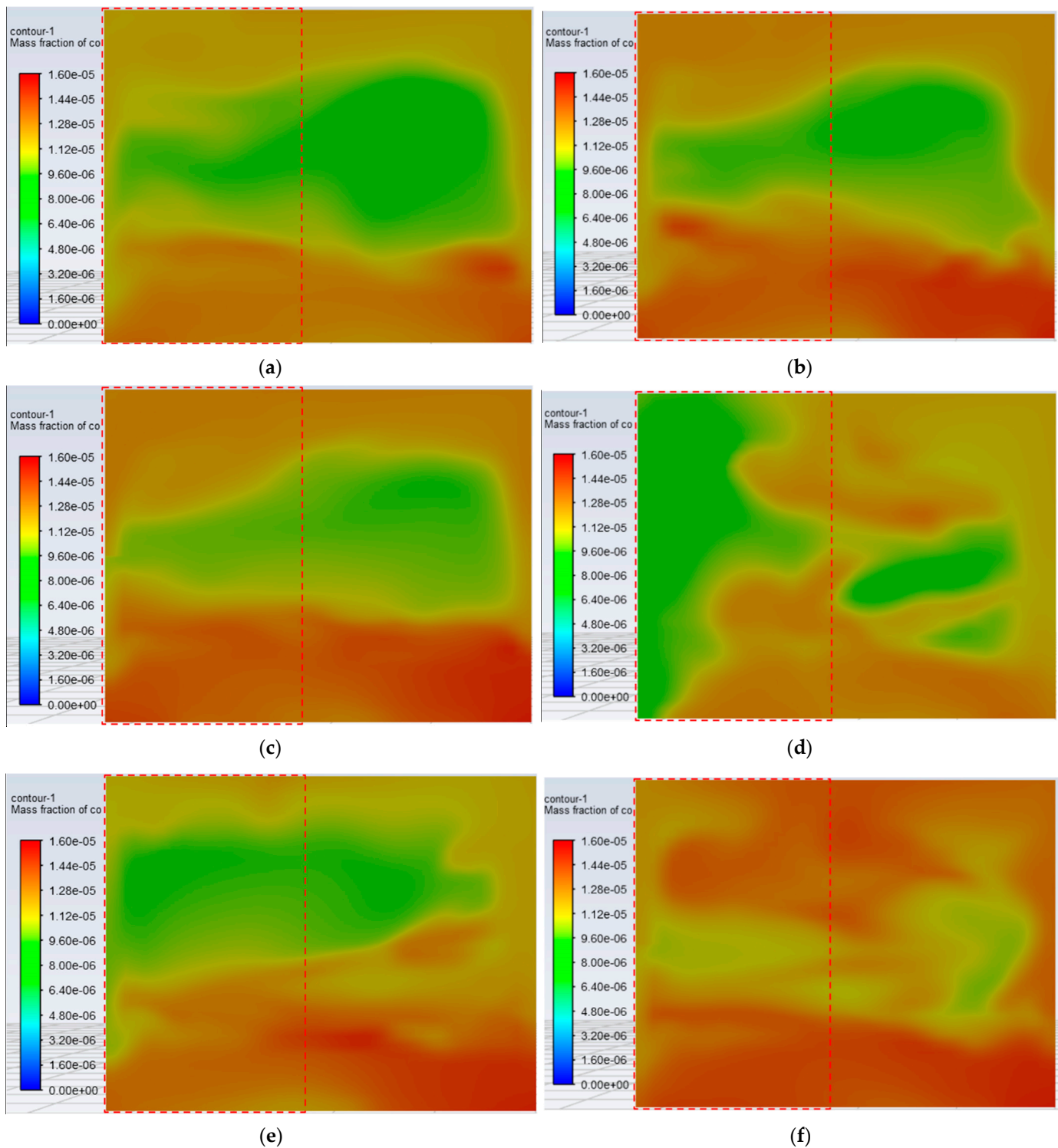


**Figure 13.** Contours of indoor 1.2 m high plane CO concentration distribution under six schemes: (a) MOUSLE, (b) MSUSLE, (c) MUSEWP, (d) DOUSLE, (e) DSUSLE, (f) DUSEWP.

When the air supply volume is  $Q = 141 \text{ m}^3/\text{h}$ , the supply air temperature is set as  $8.4 \text{ }^\circ\text{C}$  according to the FGFAHE experimental results. The ventilation simulation of the room is carried out in the above six ventilation schemes. The temperature distribution contours are generated by intercepting the plane at the height of 1.2 m in the room, and the area where the kang is located is marked with a red frame, as shown in Figure 14.

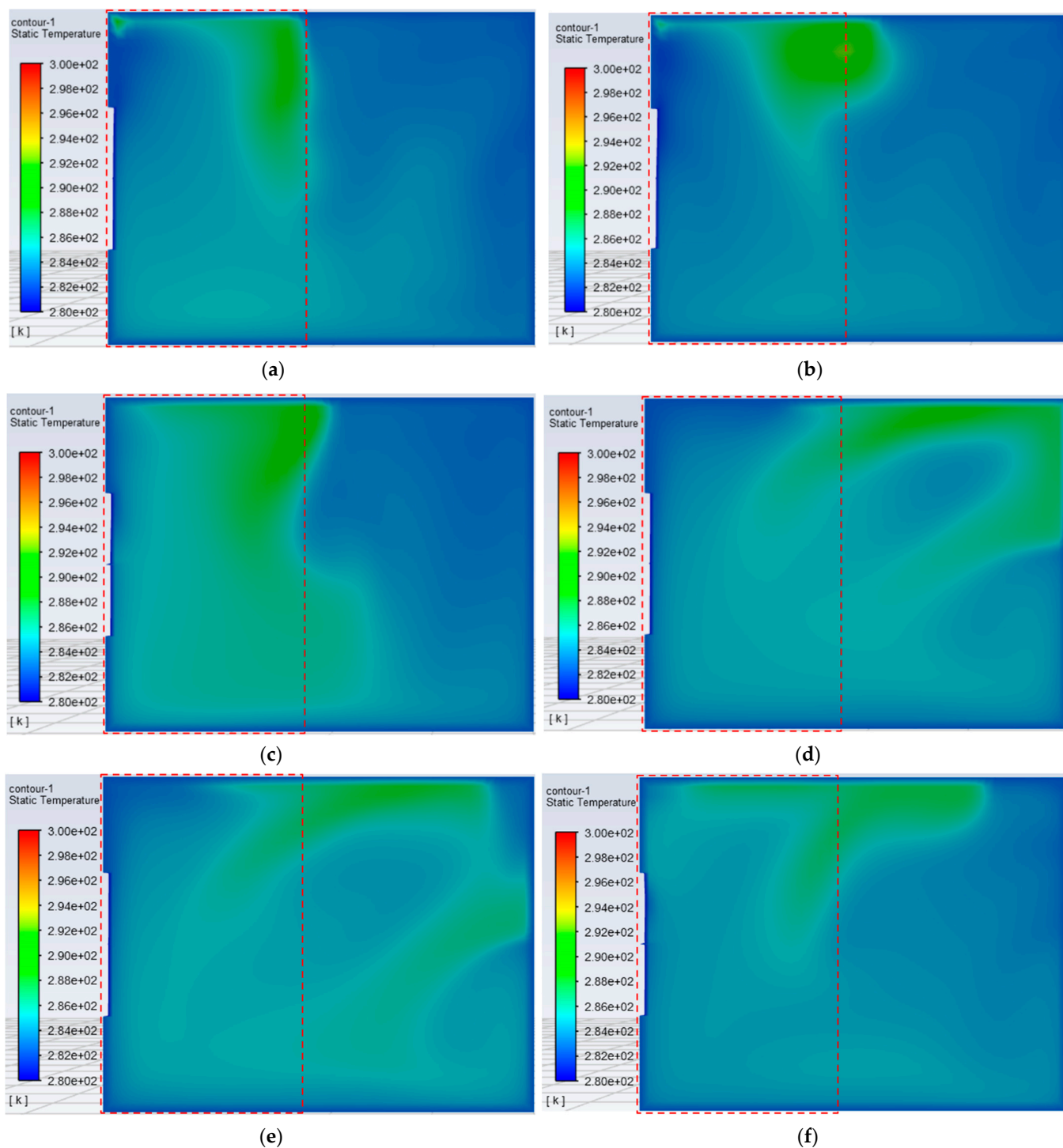


**Figure 14.** Contours of indoor 1.2 m high plane temperature distribution under six schemes: (a) MOUSLE, (b) MSUSLE, (c) MUSEWP, (d) DOUSLE, (e) DSUSLE, (f) DUSEWP.

It can be found through calculation that the indoor air temperature is reduced by an average of 1.3 °C when the above six ventilation schemes are used for ventilation. It can be seen from Figure 14 that when the three ventilation methods of median air supply are used, the areas with higher temperature are mainly distributed on the kang side. Calculating the air temperature of the area where the kang is located and the area where the floor is located, a table is drawn, as shown in Table 6. It can be found that the temperature of the area where the kang is located is 0.63 °C higher when the three median air supply schemes are used than when the three diagonal air supply schemes are used. That is to say, the use of

these three ventilation methods of median air supply can reduce the impact of insufficient preheated fresh air on the occupants' comfort.

**Table 6.** The average temperature of the air on the kang side and the floor side when the ventilation volume is  $Q = 141 \text{ m}^3/\text{h}$ .

	MOUSLE	MSUSLE	MUSEWP	DOUSLE	DSUSLE	DUSEWP
Kang side	285.65 K	285.95 K	285.40 K	284.92 K	285.06 K	285.14 K
Floor side	283.94 K	283.79 K	284.69 K	285.00 K	285.27 K	284.88 K

The air flow rate should not be too high in the areas where people need to stay indoors for a long time, otherwise it will cause discomfort to the people and even affect the daily activities of residents. It is required in the “Design Code for Heating Ventilation and Air Condition of civil buildings (GB50736-2012)” that the average air velocity of indoor activity areas of the buildings with hot air heating in winter should not be greater than 0.3 m/s, and the average indoor air velocity of air conditioning in indoor long-term stay areas in winter should not be greater than 0.2 m/s.

A plane with a height of 1.2 m to generate a contour of air velocity distribution is shown in Figure 15. The speed range in the contour is 0–1.3 m/s. It can be seen from the figure that under the six ventilation modes, most of the area where the kang is located has an air velocity exceeding 0.3 m/s, and the air velocity near the south side wall of the bedroom reaches nearly 1.3 m/s. The air velocity of the area is calculated for where the kang is located and where the floor is located, and a table is drawn, as shown in Table 7. It can be found that the average air velocity in the area where the kang is located reaches more than 0.35 m/s. Therefore, when high air volume is required for ventilation, it is recommended to turn off or switch the ventilation mode as soon as possible after diluting the indoor air pollutants.

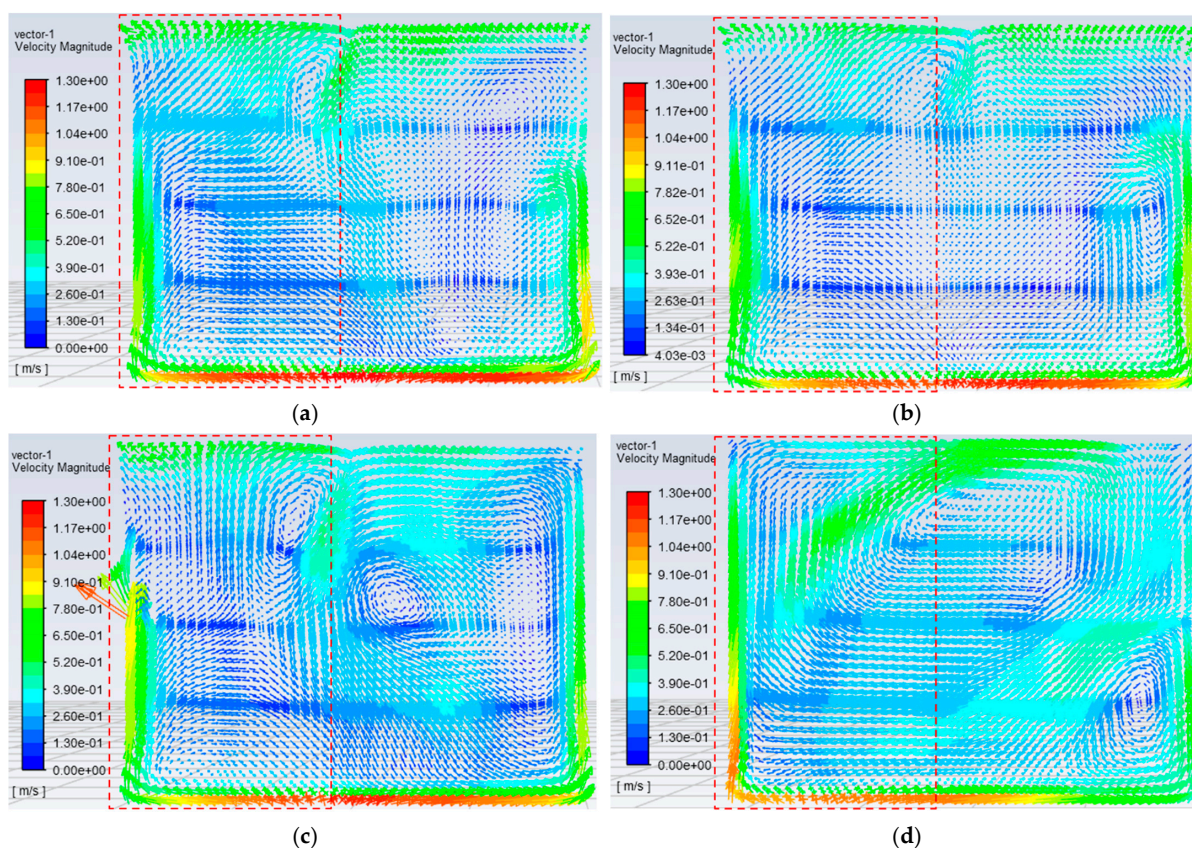


**Figure 15.** Cont.

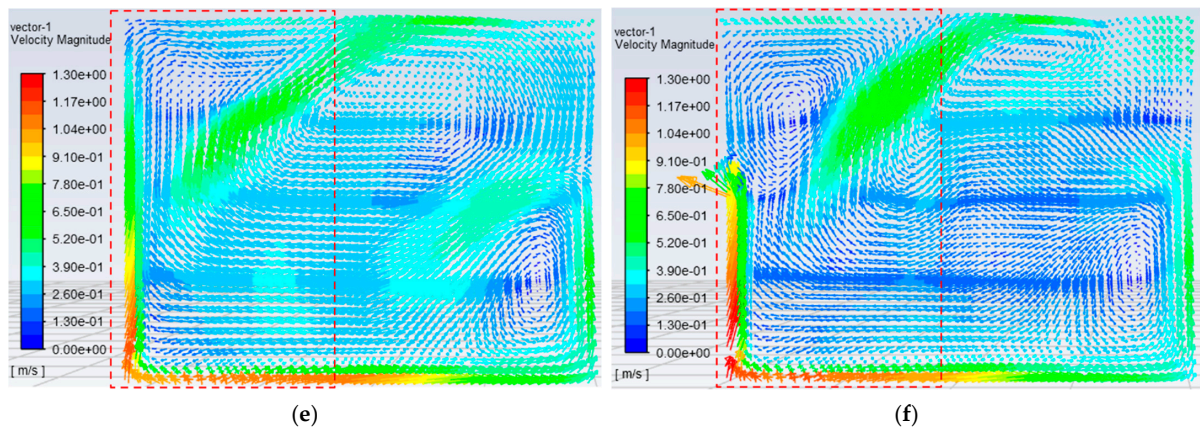


**Figure 15.** Contours of indoor 1.2 m high plane air velocity distribution under six schemes: (a) MOUSLE, (b) MSUSLE, (c) MUSEWP, (d) DOUSLE, (e) DSUSLE, (f) DUSEWP.

**Table 7.** The average air velocity on the kang side and the floor side when the ventilation volume is  $Q = 141 \text{ m}^3/\text{h}$ .

	MOUSLE	MSUSLE	MUSEWP	DOUSLE	DSUSLE	DUSEWP
Kang side	0.35 m/s	0.35 m/s	0.37 m/s	0.35 m/s	0.35 m/s	0.31 m/s
Floor side	0.38 m/s	0.37 m/s	0.38 m/s	0.33 m/s	0.31 m/s	0.26 m/s

When the air supply volume is  $Q = 29 \text{ m}^3/\text{h}$ , referring to the FGFAHE experimental results, the air supply temperature is set to  $30.12 \text{ }^\circ\text{C}$ . The ventilation simulation of the room is carried out as in the above six ventilation schemes. The temperature distribution contours are generated by intercepting the plane at a height of 1.2 m in the room, and the area where the kang is located is marked with a red frame, as shown in Figure 16.

The calculation shows that the indoor temperature will increase by  $1.0 \text{ }^\circ\text{C}$  on average when the above six ventilation schemes are used for ventilation. It can be seen from Figure 16 that when the three ventilation methods of median air supply are adopted, the areas with higher temperature are mainly distributed on the kang side. The air temperature of the area is calculated where the kang is located and where the floor is located, and a table is drawn, as shown in Table 8. It can be found that the temperature of the area where the kang is located is  $2.07 \text{ }^\circ\text{C}$  higher when the three median air supply schemes are used than when the three diagonal air supply schemes are used. That is, the use of these three ventilation methods can improve the thermal comfort of the occupants to a greater extent. A plane with a height of 1.2 m is taken to generate contours of air velocity distribution, as shown in Figure 17.

**Table 8.** The average temperature of the air on the kang side and the floor side when the ventilation volume is  $Q = 29 \text{ m}^3/\text{h}$ .

	MOUSLE	MSUSLE	MUSEWP	DOUSLE	DSUSLE	DUSEWP
Kang side	291.12 K	290.75 K	291.67 K	288.97 K	288.89 K	289.45 K
Floor side	286.88 K	286.59 K	286.04 K	287.00 K	286.99 K	286.44 K

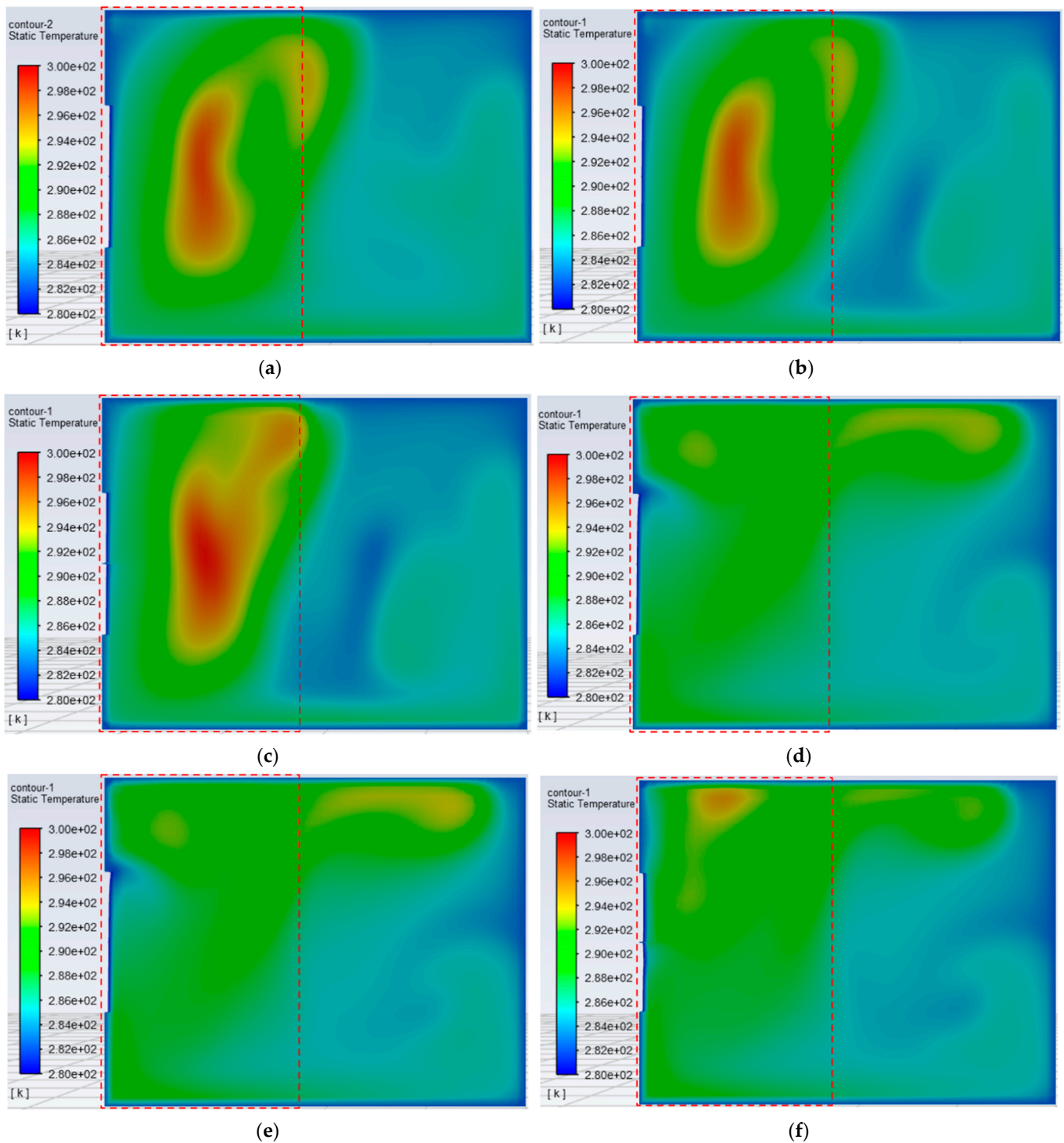


**Figure 16.** Contours of indoor 1.2m high plane temperature distribution under six schemes: (a) MOUSLE, (b) MSUSLE, (c) MUSEWP, (d) DOUSLE, (e) DSUSLE, (f) DUSEWP.

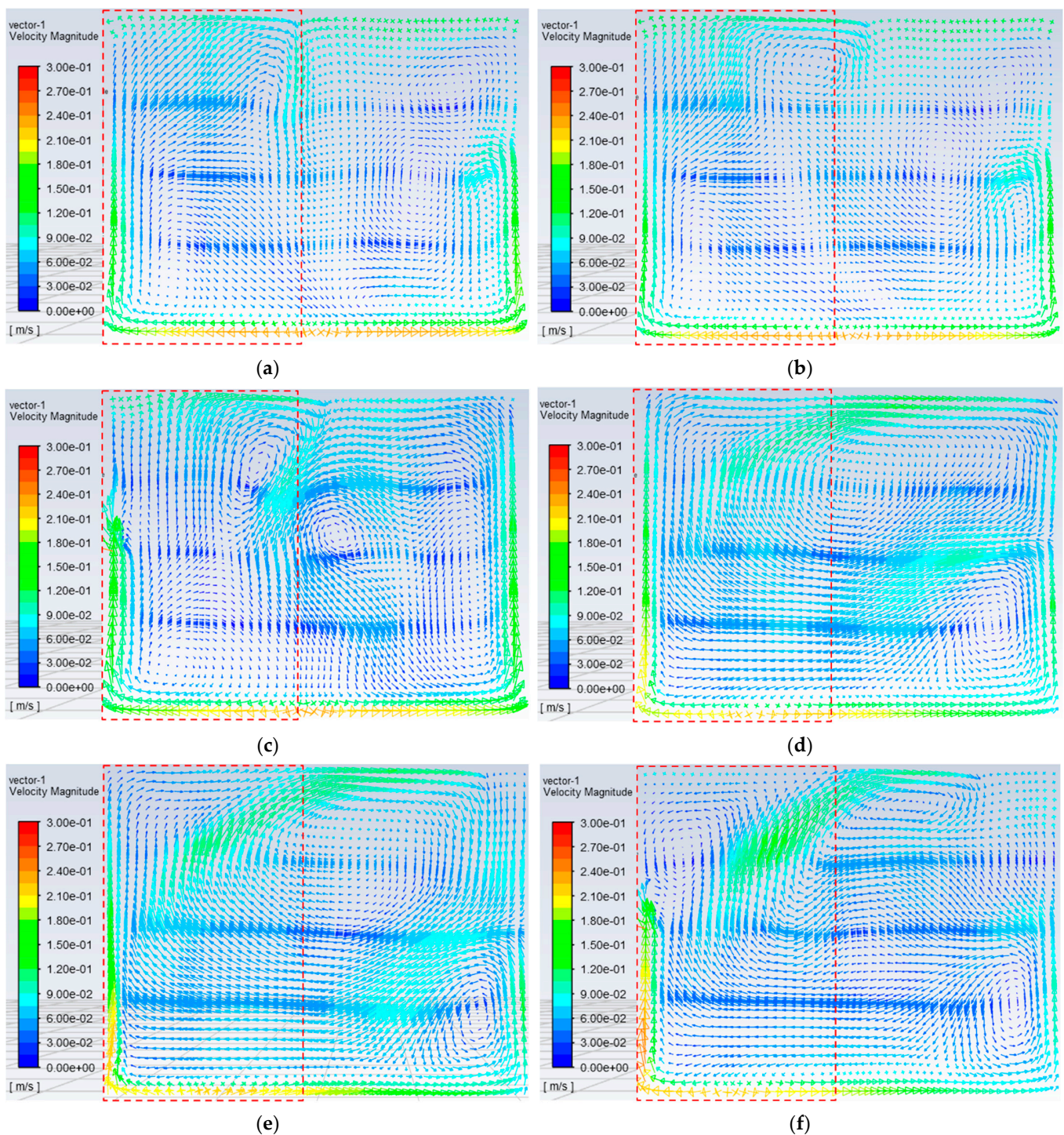


**Figure 17.** Contours of indoor 1.2 m high plane air velocity distribution under six schemes: (a) MOUSLE, (b) MSUSLE, (c) MUSEWP, (d) DOUSLE, (e) DSUSLE, (f) DUSEWP.

The velocity range in the contours is 0–0.3 m/s. It can be seen from Figure 17 that under the six ventilation modes, there are some areas where the air velocity is higher than 0.2 m/s, but lower than 0.3 m/s, mainly distributed near the inner wall on the south side of the bedroom. Most of the air velocity in the area where the kang is located is lower than 0.2 m/s. Such air velocity would not cause discomfort to indoor occupants. The air velocity of the area where the kang is located and the area where the floor is located is calculated, and a table is drawn, as shown in Table 9. It can be found that the average air velocity in

the area where the kang is located reaches about 0.06 m/s. It can be ventilated for a long time in this state.

**Table 9.** The average air velocity on the kang side and the floor side when the ventilation volume is  $Q = 29 \text{ m}^3/\text{h}$ .

	MOUSLE	MSUSLE	MUSEWP	DOUSLE	DSUSLE	DUSEWP
Kang side	0.05 m/s	0.04 m/s	0.03 m/s	0.08 m/s	0.06 m/s	0.09 m/s
Floor side	0.03 m/s	0.02 m/s	0.01 m/s	0.08 m/s	0.1 m/s	0.08 m/s

## 5. Conclusions

In this study, indoor  $\text{CO}_2$ , CO,  $\text{PM}_{10}$ ,  $\text{PM}_{2.5}$ , formaldehyde, TVOC, temperature and relative humidity are measured in three typical houses in a rural area of Chaoyang City, Liaoning Province, China. A FGFAHE experiment bench is built and ventilation experiments are carried out. Six ventilation schemes, namely MOUSLE, MSUSLE, MUSEWP, DOUSLE, DSUSLE, DUSEWP, are proposed, and their effects on indoor CO dilution and indoor thermal environment in farmhouses are explored by means of simulation. The conclusions of the study are as follows.

- (1) The air pollutants such as  $\text{CO}_2$ , CO,  $\text{PM}_{2.5}$  and  $\text{PM}_{10}$  in the bedrooms of the farmhouses seriously exceed the standard. Between 7:00 and 22:00, the concentrations of  $\text{CO}_2$  and CO are in a state of exceeding or close to the standard most of the time. The average excess multiples of  $\text{PM}_{2.5}$  and  $\text{PM}_{10}$  are 4.2 and 5.7. Between 22:00 and 7:00, the concentration of  $\text{CO}_2$  continued to exceed the standard, and the concentrations of CO,  $\text{PM}_{2.5}$  and  $\text{PM}_{10}$  are within the standard value for most of the time. Formaldehyde and TVOC levels do not exceed the standard throughout the day, and their average concentrations are far lower than the standard value. Relative humidity is within the standard range for most of the day. The bedroom temperature shows a trend of rising first and then falling between 7:00 and 22:00, and the average temperature is lower than the design temperature of farmhouses.
- (2) The biomass combustion flue gas can preheat the outdoor air from  $-17^\circ\text{C}$ – $-10^\circ\text{C}$  to  $6^\circ\text{C}$ – $30^\circ\text{C}$  during the time of burning. The mechanical air supply and external window infiltration can effectively dilute the indoor CO of farmhouses, and the dilution rate is more than double that of natural infiltration. When the ventilation volume is  $29 \text{ m}^3/\text{h}$ – $141 \text{ m}^3/\text{h}$ , it only takes about 17–30 min to reduce the CO concentration of  $20 \text{ mg}/\text{m}^3$ – $25 \text{ mg}/\text{m}^3$  to below the standard value ( $10 \text{ mg}/\text{m}^3$ ).
- (3) All six of the ventilation schemes have a good dilution effect on indoor CO. When the ventilation is carried out with DOUSLE, the indoor CO dilution is the fastest and the CO concentration in the area near the kang is the lowest. When the bedroom is ventilated with three central air supply schemes, the thermal environment in the area where the kang is located is the best. Ventilation with a high ventilation volume will cause the indoor air temperature to drop and the flow velocity to increase, causing discomfort to indoor occupants. When the ventilation is performed with low air volume, the supply air temperature is higher than the indoor air temperature and has little influence on the indoor velocity field, which can improve indoor thermal environment.

**Author Contributions:** Conceptualization, B.Z. and X.C.; methodology, X.C.; formal analysis, M.L.; investigation, X.C.; writing—original draft preparation, X.C.; writing—review and editing, B.Z.; supervision, M.L. All authors have read and agreed to the published version of the manuscript.

**Funding:** This research received no external funding.

**Institutional Review Board Statement:** Not applicable.

**Informed Consent Statement:** Not applicable.

**Data Availability Statement:** Not applicable.



**Conflicts of Interest:** The authors declare no conflict of interest.

### Nomenclature

SKS	Stove and Kang System
TVOC	Total Volatile Organic Compounds
PAP	Personnel Activity Period (7:00–22:00)
NSP	Nighttime Sleep Period (22:00–7:00)
FGFAHE	Flue Gas-Fresh Air Heat Exchange
MOUSLE	Median Opposite Side Upper Air Supply and Lower Exhaust Air
MSUSLE	Median Same Side Upper Air Supply and Lower Exhaust Air
MUSEWP	Median Upper Air Supply and Exterior Window Penetration
DOUSLE	Diagonal Opposite Side Upper Air Supply and Lower Exhaust Air
DSUSLE	Diagonal Same Side Upper Air Supply and Lower Exhaust Air
DUSEWP	Diagonal Upper Air Supply and Exterior Window Penetration

### References

- Zhang, Y.; Zhang, Y.; Wang, Z.C. Analysis of indoor air pollution in rural residences in northern China. *Chem. Adhes.* **2018**, *40*, 461–463.
- Ji, W.H.; Luo, Q.; Zhang, J.L.; Wang, H.H.; Du, T.; Heiselberg, P.K. Investigation on thermal performance of the wall-mounted attached ventilation for night cooling under hot summer conditions. *Build. Environ.* **2018**, *146*, 268–279. [[CrossRef](#)]
- Gao, X.X.; Liu, J.P.; Hu, R.R.; Akashi, Y.; Sumiyoshi, D. A simplified model for dynamic analysis of the indoor thermal environment of rooms with a Chinese kang. *Build. Environ.* **2017**, *111*, 265–278. [[CrossRef](#)]
- Huo, H.M.; Xu, W.; Li, A.G. Comparison and analysis of envelope structure retrofitting schemes for rural residential building in Northern China based on entropy method. *Build. Sci.* **2019**, *35*, 57–64.
- Guo, Y.M.; Zeng, H.M.; Zheng, R.S.; Li, S.S.; Barnett, A.G.; Zhang, S.W.; Zou, X.N.; Huxley, R.; Chen, W.Q.; Williams, G. The association between lung cancer incidence and ambient air pollution in China: A spatiotemporal analysis. *Environ. Res.* **2016**, *144*, 60–65. [[CrossRef](#)]
- Kilabuko, J.H.; Matsuki, H.; Nakai, S. Air quality and acute respiratory illness in biomass fuel using homes in Bagamoyo, Tanzania. *Int. J. Environ. Res. Public Health* **2007**, *4*, 39–44. [[CrossRef](#)] [[PubMed](#)]
- Chen, Y.C.; Fei, J.; Sun, Z.; Shen, G.F.; Du, W.; Yang, L.Y.; Wu, R.X.; Chen, A.; Zhao, M.R. Household air pollution from cooking and heating and its impacts on blood pressure in residents living in rural cave dwellings in Loess Plateau of China. *Environ. Sci. Pollut. Res.* **2020**, *27*, 36677–36687. [[CrossRef](#)]
- Xue, Q.W.; Wang, Z.J.; Liu, J.; Dong, J.K. Indoor PM<sub>2.5</sub> concentrations during winter in a severe cold region of China: A comparison of passive and conventional residential buildings. *Build. Environ.* **2020**, *180*, 106857. [[CrossRef](#)]
- Wang, Z.J.; Xie, D.D.; Tang, R. Indoor air pollutions and their correlation at rural houses in severe cold region in winter. *J. Harbin Inst. Technol.* **2014**, *46*, 60–64.
- Zhang, X.Y.; Chen, B. Analysis on the PM<sub>2.5</sub> Concentration During Heating and Cooking in Cold Rural Areas of Northern China. In Proceedings of the 4th International Conference on Sustainable Energy and Environmental Engineering, Shenzhen, China, 20–21 December 2013; Atlantis Press: Shenzhen, China; pp. 1083–1086.
- Gu, Q.P.; Gao, X.; Chen, Y.; Yu, Q.; Zhang, Y.; Chen, L.M. The Mass Concentration Characters of Indoor PM<sub>2.5</sub> in Rural Areas in Jiangsu Province. *J. Fudan Univ.* **2009**, *48*, 593–597.
- Yang, Z. Reserach on the Improvement of Indoor Air Quality and Strategies of Ventilation for Rural Houses in Cold Region. Master’s Thesis, Harbin Institute of Technology, Harbin, China, 2009.
- Liu, C.L. Research on Indoor Air Quality at Rural Residential House in Northeast. Master’s Thesis, Harbin Engineering University, Harbin, China, 2007.
- Yang, X.B.; Jin, X.Q.; Du, Z.M.; Fan, B.; Chai, X.F. Evaluation of four control strategies for building VAV air-conditioning systems. *Energy Build.* **2011**, *43*, 414–422. [[CrossRef](#)]
- Collett, C.W.; Ross, J.A.; Sterling, E.M. Quality assurance strategies for investigating IAQ problems. *ASHRAE J. Am. Soc. Heat. Refrig. Air Cond. Eng.* **1994**, *36*, 42.
- Hagerhed-Engman, L.; Sigsgaard, T.; Samuelson, L.; Sundell, J.; Janson, S.; Bornehag, C.G. Low home ventilation rate in combination with moldy odor from the building structure increase the risk for allergic symptoms in children. *Indoor Air* **2009**, *19*, 184–192. [[CrossRef](#)]
- Wang, H.Q. *Ventilation Engineering*, 1st ed.; China Machine Press: Beijing, China, 2007; p. 17.
- Zhang, K.; Ren, L.; Wang, N.X. Analysis on nature ventilation design of residential buildings in northern towns. *J. Shenyang Jianzhu Univ. (Soc. Sci.)* **2011**, *13*, 274–277.
- Zhai, X.Q.; Song, Z.P.; Wang, R.Z. A review for the applications of solar chimneys in buildings. *Renew. Sustain. Energy Rev.* **2011**, *15*, 3757–3767. [[CrossRef](#)]

20. Elghamry, R.; Hassan, H. Experimental investigation of building heating and ventilation by using Trombe wall coupled with renewable energy system under semi-arid climate conditions. *Sol. Energy* **2020**, *201*, 63–74. [[CrossRef](#)]
21. Calautit, J.K.; O'Connor, D.; Tien, P.W.; Wei, S.Y.; Pantua, C.A.J.; Ben, H. Development of a natural ventilation windcatcher with passive heat recovery wheel for mild-cold climates: CFD and experimental analysis. *Renew. Energy* **2020**, *160*, 465–482. [[CrossRef](#)]
22. Ye, W.; Zhang, X.; Gao, J.; Gao, G.Y.; Zhou, X.; Su, X. Indoor air pollutants, ventilation rate determinants and potential control strategies in Chinese dwellings: A literature review. *Sci. Total Environ.* **2017**, *586*, 696–729. [[CrossRef](#)]
23. Mijakowski, M.; Sowa, J. An attempt to improve indoor environment by installing humidity sensitive air inlets in a naturally ventilated kindergarten building. *Build. Environ.* **2017**, *111*, 180–191. [[CrossRef](#)]
24. Leung, D.Y.C. Outdoor-indoor air pollution in urban environment: Challenges and opportunity. *Front. Environ. Sci.* **2015**, *2*, 69. [[CrossRef](#)]
25. Zhao, X.Y. Research on the Natural Ventilation Design of the Residence in Nangjing. Master's Thesis, Southeast University, Nanjing, China, 2005.
26. Niculita-Hirzel, H.; Yang, S.; Jörin, C.H.; Perret, V.; Licina, D.; Pernot, J.G. Fungal Contaminants in Energy Efficient Dwellings: Impact of Ventilation Type and Level of Urbanization. *Int. J. Environ. Res. Public Health* **2020**, *17*, 4936. [[CrossRef](#)] [[PubMed](#)]
27. Elkilani, A.; Bouhamra, W. Estimation of optimum requirements for indoor air quality and energy consumption in some residences in Kuwait. *Environ. Int.* **2001**, *27*, 443–447. [[CrossRef](#)]
28. Joo, J.; Zheng, Q.; Lee, G.; Kim, J.T.; Kim, S. Optimum energy use to satisfy indoor air quality needs. *Energy Build.* **2012**, *46*, 62–67. [[CrossRef](#)]
29. Shen, H.T. Research on Suitable Ventilation Mode in Rural Housing of Northern Region in Heating Season. Master's Thesis, Harbin Institute of Technology, Harbin, China, 2014.
30. Zhao, J.X.; An, B.Y.; Ma, Y.F.; Liu, X.Y.; Liu, S.N.; Liu, L. Research on the design of energy-saving ventilation system for farm buildings. *Sci. Technol. Innov.* **2020**, *5*, 90–91.
31. Wang, Q.; Ploskic, A.; Song, X.Q.; Holmberg, S. Ventilation heat recovery jointed low-temperature heating in retrofitting—An investigation of energy conservation, environmental impacts and indoor air quality in Swedish multifamily houses. *Energy Build.* **2016**, *121*, 250–264. [[CrossRef](#)]
32. Chen, C.Y.; Yao, C.S.; Li, M. Analysis of rural residential energy consumption and its carbon emission in China, 2001–2010. *Renew. Energy Resour.* **2012**, *30*, 121–127.
33. Jin, X. Flow and Heat Transfer Analysis of Flue Gas in Flue Composite Wall in Northern Rural Areas. Master Thesis, Harbin Institute of Technology, Harbin, China, 2018.
34. Yu, K.C.; Tan, Y.F.; Zhang, T.T.; Jin, X.; Zhang, J.D.; Wang, X.M. Experimental and simulation study on the thermal performance of a novel flue composite wall. *Build. Environ.* **2019**, *151*, 126–139. [[CrossRef](#)]
35. Jin, X.; Tan, Y.F.; Yu, K.C. Test and analysis of the thermal performance of combined elevated kang and radiator heating system in northern rural areas. *J. Harbin Inst. Technol.* **2019**, *51*, 179–186.
36. Zhao, Y.B. Research on Tunnel-Type Heating System Using Fuel Gas Heat in Northern Rural House. Master's Dissertation, Harbin Institute of Technology, Harbin, China, 2014.
37. Kim, J.; Hong, T.; Lee, M.; Jeong, K. Analyzing the real-time indoor environmental quality factors considering the influence of the building occupants' behaviors and the ventilation. *Build. Environ.* **2019**, *156*, 99–109. [[CrossRef](#)]
38. Guyot, G.; Sherman, M.H.; Walker, I.S. Smart ventilation energy and indoor air quality performance in residential buildings: A review. *Energy Build.* **2018**, *165*, 416–430. [[CrossRef](#)]
39. Lu, Y.Q. *Practical Heating and Air Conditioning Design Handbook*, 2nd ed.; China Architecture & Building Press: Beijing, China, 2007; pp. 1099–1138.
40. Wang, H.Q. *Ventilation Engineering*; Machinery Industry Press: Beijing, China, 2007; pp. 41–42.